Structure and Function of the GTP Binding Protein Gtr1 and Its Role in Phosphate Transport in *Saccharomyces cerevisiae*†

Jens O. Lagerstedt,‡,§ Ian Reeve,|| John C. Voss,|| and Bengt L. Persson*,‡,§

Department of Biochemistry and Biophysics, Arrhenius Laboratory, Stockholm University, S-106 91 Stockholm, Sweden, Department of Chemistry and Biomedical Sciences, Kalmar University, S-391 29 Kalmar, Sweden, and Department of Biological Chemistry, University of California School of Medicine, Davis, California 95616

Received June 27, 2004; Revised Manuscript Received October 17, 2004

ABSTRACT: The Pho84 high-affinity phosphate permease is the primary phosphate transporter in the yeast *Saccharomyces cerevisiae* under phosphate-limiting conditions. The soluble G protein, Gtr1, has previously been suggested to be involved in the derepressible Pho84 phosphate uptake function. This idea was based on a displayed deletion phenotype of Δ*gtr1* similar to the Δ*pho84* phenotype. As of yet, the mode of interaction has not been described. The consequences of a deletion of *gtr1* on *in vivo* Pho84 expression, trafficking and activity, and extracellular phosphatase activity were analyzed in strains synthesizing either Pho84−green fluorescent protein or Pho84−myc chimeras. The studies revealed a delayed response in Pho84-mediated phosphate uptake and extracellular phosphatase activity under phosphate-limiting conditions. EPR spectroscopic studies verified that the N-terminal G binding domain (residues 1−185) harbors the nucleotide responsive elements. In contrast, the spectra obtained for the C-terminal part (residues 186−310) displayed no evidence of conformational changes upon GTP addition.

Inorganic phosphate is an essential nutrient for cell survival. In the yeast *Saccharomyces cerevisiae*, several protein components have been shown to be directly or indirectly involved in the active uptake of this molecule across the plasma membrane (reviewed in ref *1*). Among these are the gene products of *PHO84* (*2*) and *GTR1* (*3*). The Pho84 protein is the major high-affinity phosphate transporter in *S. cerevisiae*, which consists of 12 putative transmembrane segments and belongs to the major facilitator superfamily (MFS)[1] (*4*). Under phosphate-limiting conditions, the *PHO84* gene is derepressed (*5*) and the synthesized Pho84 protein is routed to the plasma membrane (*6*), a location at which the Pho84 is active in proton-coupled high-affinity phosphate transport. Although several studies have shown that the Pho84 solely is competent in phosphate transport in reconstituted *in vitro* systems (*7*−*9*), other results have demonstrated that the absence of the *GTR1* gene diminishes the high-affinity phosphate uptake capacity of the yeast cells and also makes the growth of the cells temperature-sensitive (*3*). The soluble Gtr1 protein belongs to the Ras family of small GTP-binding proteins. One characteristic of G proteins is their function as molecular switches, active in the GTP-bound state and inactive in the GDP-bound state (*10*). They all contain highly conserved guanine nucleotide binding motifs (*11*), which are also present in the Gtr1 protein (*12*, *13*). Gtr1 has been reported to bind both GDP and GTP, with a preference for the latter, as demonstrated in competition experiments by use of radioactive nucleotides (*13*). Interestingly, in guanine nucleotide binding motif G4 (consensus NKxD), the asparagine is replaced with a histidine (residue H126). Furthermore, Gtr1 has an additional C-terminal domain of unknown function. These special properties of the Gtr1 protein have led to the introduction of a novel subclass of the Ras family of small G proteins in addition to the existing Ras, Ran, Rho, Rab, and ARF branches (*12*, *13*). This new subclass is shared with another *S. cerevisiae* protein, Gtr1 homologue Gtr2, and also with a number of mammalian proteins, the RagA and RagB proteins (*12*). Both RagA and RagB are capable of restoring the temperature sensitivity of Δ*gtr1* cells (*14*).

Gtr1-HA induced by the galactose promoter has, by immunofluorescence microscopy analysis, been shown to be localized within the cytoplasm and, to a lesser extent, in the nucleus (*15*).

In vitro pull-down assays have demonstrated that the Gtr1 protein is required for self-interaction in the Gtr2 protein. It has been suggested that, through this interaction, Gtr1 regulates the GTP/GDP state of the Gsp1 protein (*13*), a yeast Ran protein. Recently, a yeast two-hybrid analysis showed that Gtr1 interacts with Nop8 (*16*), an essential nucleolar protein involved in ribosome biogenesis (*17*). Clearly, Gtr1 serves a number of functions in the yeast cell.

† Supported by Human Frontier Science Organization Grant RG00281/2000-M, Swedish Research Council Grant 621-2003-3558, and travel fellowship awards to J.O.L. from the Swedish Foundation for International Cooperation in Research and Higher Education, the Foundation Blanceflor Boncompagni-Ludovisi, née Bildt, the foundation Bengt Lundqvist Minne, and AstraZeneca.

* To whom correspondence should be addressed. Phone: (0046) 480 446276. Fax: (0046) 480 446262. E-mail: bengt.persson@hik.se.

‡ Stockholm University.

§ Kalmar University.

|| University of California.

[1] Abbreviations: ER, endoplasmic reticulum; EPR, electron paramagnetic resonance; HA, heme agglutinin; HP_i, high-phosphate medium; IPTG, isopropyl 1-thio-β-D-galactopyranoside; LP_i, low-phosphate medium; MFS, major facilitator superfamily; MTS, (1-oxyl-2,2,5,5-tetramethylpyrroline-3-methyl)methanethiosulfonate; PMSF, phenylmethanesulfonyl fluoride; TCEP, tris(2-carboxyethyl)phosphine.

10.1021/bi048659v CCC: $30.25
Published on Web 12/17/2004

Table 1

construct[a]	amino acids	mutations
FL-Gtr1^{WT}	1−310	none
NT-Gtr1^{WT}	1−185	stop after amino acid 185
CT-Gtr1^{WT}	186−310	start at amino acid 186
FL-Gtr1$^{single\ C62}$	1−310	C180S, C217S, C257S, C284S
FL-Gtr1$^{single\ C180}$	1−310	C62S, C217S, C257S, C284S
FL-Gtr1$^{cysteine-free}$	1−310	C62S, C180S, C217S, C257S, C284S
FL-Gtr1$^{single\ V37C}$	1−310	C62S, C180S, C217S, C257S, C284S, V37C
FL-Gtr1$^{single\ R67C}$	1−310	C62S, C180S, C217S, C257S, C284S, R67C
NT-Gtr1$^{single\ C180}$	1−185	C62S, stop after amino acid 185
FL-Gtr1$^{single\ C62,\ H126N}$	1−310	H126N, C180S, C217S, C257S, C284S
FL-Gtr1$^{single\ C62,\ H126K}$	1−310	H126K, C180S, C217S, C257S, C284S

[a] Abbreviations: FL, full-length; NT, N-terminal domain; CT, C-terminal domain.

The aim of this study was to investigate the involvement of Gtr1 in Pho84-mediated high-affinity phosphate uptake and also to study structural and functional properties of the Gtr1 protein. Constructed Δ*gtr1* yeast strains were cultivated under phosphate-limiting conditions and compared with similarly grown *GTR1*$^+$ strains for phosphate uptake capability, extracellular phosphatase activity, and Pho84−green fluorescent protein (Pho84−GFP) localization. We employed electron paramagnetic resonance (EPR) spectroscopy on the spin-labeled protein to further analyze the conformational response of sites accessible to nucleotide binding.

EXPERIMENTAL PROCEDURES

Materials and Strains. A thio-specific nitroxide spin-label [MTS-SL, (1-oxyl-2,2,5,5-tetramethylpyrroline-3-methyl)-methanethiosulfonate] was purchased from Reanal Finechemical (Budapest, Hungary). [^{32}P]Orthophosphate (carrier-free), horseradish peroxidase-conjugated anti-mouse Ig antibody (from sheep), and the enhanced chemiluminescence detection kit were obtained from Amersham Bioscience. Anti-Xpress antibody, plasmid pTrcHisB, and *Escherichia coli* TOP10F′ cells were obtained from Invitrogen. Expand High Fidelity polymerase was from Roche. Zymolyase 100T was obtained from Seikagaku America, Inc. All mutagenic primers were purchased from TAG (Copenhagen A/S, Denmark). Cybergene AB and Davis Sequencing performed DNA sequence determination.

Plasmids. The *GTR1* gene was PCR amplified from genomic *S. cerevisiae* DNA and cloned into expression plasmid pTrcHisB by use of *Bam*HI and *Eco*RI restriction sites. The resulting plasmid, pTrcHisB/GTR1^{WT}, expressing Gtr1 with an N-terminal tag of six consecutive histidines and the Xpress antibody epitope, was used as template for subsequent *GTR1* mutant constructions (Table 1).

GFP Tagging of PHO84 and Deletion of GTR1. Chromosomal *PHO84* was tagged with the *GFP* gene in the haploid, prototrophic *S. cerevisiae* CEN.PK113-5D (*MAT*a *MAL2-8c SUC2 ura3-52*) strain as described previously (*6*). The *GTR1* gene was subsequently deleted in the constructed strain, CEN.PK113-5D/Pho84^{WT}-GFP, and also in CEN-.PK113-5D/Pho84^{WT}-MYC cells (*18*) using PCR technology (*19*). The *URA3* cassette used for *GTR1* gene deletion was PCR amplified from pRS406 with oligonucleotide primers 5′-GAAACTGCTTCTGATGGGCCGGTCCGGCTCCGG-TAAATCGTCAATGTATCACGAGGCCCTTTCGTC and 5′-CTTTTTTGATGTTTTCCAATACTAATTCTTGTGG-AATATTCATATACGTTTACAATTTCCTGATGCGG and subsequently transformed (*20*) into cells wherein homologous recombination occurred. The constructed strains were selected either on YPD-Geneticin (200 μg/mL) or on synthetic complete (−Ura) plates, after which colonies were restreaked on fresh plates and positives were verified using qualitative PCR, Western blot, and/or GFP fluorescence.

Growth and Expression. S. cerevisiae cells expressing Pho84−MYC or Pho84−GFP in either *GTR1*$^+$ or Δ*gtr1* background were precultivated aerobically for 12 h in YPD medium at 30 °C, washed twice with water, and inoculated in high-phosphate (HP_i) or low-phosphate (LP_i) medium (*21*). Cells were grown aerobically at 30 °C. Samples for phosphate assays, Western blotting, phosphatase activity analysis, and fluorescence microscopy analyses were withdrawn at the indicated time points.

Heterologous Production and Purification. TOP10F′ *E. coli* cells were used as the host for the production of described Gtr1 variants (Table 1). Cells were induced for 6 h in Terrific Broth medium in the presence of 1 mM isopropyl 1-thio-β-D-galactopyranoside (IPTG) (full-length *GTR1* constructs) or 0.2 mM IPTG (N- and C-terminal constructs of *GTR1*), harvested, and stored at −80 °C. Cell pellets were thawed and resuspended in ice-cold buffer A [50 mM Tris buffer (pH 7.6), supplemented with 0.2 mM NaCl, 10 mM $MgCl_2$, 30 mM imidazole, 10% glycerol, and 0.1% (v/v) Triton X-100]. Tris(2-carboxyethyl)phosphine (TCEP, 100 μM) and 200 μM GDP were included in the buffers for purifications to ensure a high efficiency in binding the MTS spin-label by reducing the number of putative disulfide bridges and to obtain Gtr1−GDP proteins, respectively. The suspension was incubated with lysozyme and 1 mM phenylmethanesulfonyl fluoride (PMSF) for 40 min at 4 °C. The resulting viscous suspension was sonicated for 4 × 10 s using a micro-tip sonicator, after which the Triton X-100 concentration was increased to 0.4% and additional 1 mM PMSF was added. After a second incubation at 4 °C for 30 min followed by sonication for 4 × 10 s, the lysate was cleared by centrifugation at 100000*g* for 30 min, followed by 0.45 μm filtration. The protein extract was applied to a FPLC-connected HiTrap Chelating column (Amersham Bioscience) charged with Ni^{2+} ions. After removal of unspecifically bound proteins with an applied imidazole concentration of 150 mM in the buffer described above, His-tagged Gtr1 proteins were eluted with 500 mM imidazole. For EPR analysis, the various Gtr1 proteins at concentrations of 20 μM for the full-length mutants and 32 and 44 μM for the N- and C-terminal parts, respectively, were incubated with 200 μM MTS at 4 °C for 30 min to generate spin-labeled protein. Excess label was removed by dialysis at 4 °C (10K MWCO Slide-A-Lyzer dialysis cassette, Pierce) against buffer A, modified to contain no imidazole, TCEP, or GDP.

EPR Spectroscopy. EPR measurements were carried out in a JEOL X-band spectrometer fitted with a loop-gap resonator (*22*, *23*). An aliquot (5 μL) of purified, spin-labeled protein was placed in a sealed quartz capillary contained in

the resonator. For Gtr1 samples, spectra were acquired at room temperature (20−22 °C) or alternatively, where indicated, at 4 °C from a single 60 s scan over a field of 100 G at a microwave power of 2 mW and a modulation amplitude optimized to the natural line width of the individual spectrum (0.5−1.5 G).

Electrophoresis and Western Blot Analysis. Samples of the purified protein were mixed with sample buffer prior to separation by SDS−polyacrylamide gel electrophoresis using a 10% Laemmli system (*24*). Immunoblotting was carried out on poly(vinylidene difluoride) membranes (Immobilon-P, Millipore) according to the Western Blotting Protocol (Amersham Bioscience). Use of anti-Xpress monoclonal mouse antibody (Invitrogen) and horseradish peroxidase-conjugated anti-mouse Ig antibody (Amersham Bioscience) allowed for immunological detection of the Gtr1 proteins. After a short incubation with chemiluminescent substrates, the blot was exposed to film for 1 min.

Determinations of Phosphate Amounts. Phosphate uptake in intact *S. cerevisiae* cells expressing Pho84^{WT}−MYC in either *GTR1*$^+$ or Δ*gtr1* background grown in LP_i medium was assayed by the addition of 1 μL of [^{32}P]orthophosphate (carrier-free, 0.18 Ci/μmol, 1 mCi = 37 MBq) and phosphate to a final concentration of 0.11 mM in 30 μL aliquots of cells essentially as described previously (*5*). The extracellular phosphate concentration was determined spectrophotometrically at 850 nm essentially as described previously (*25*). Extracellular phosphatase activity was determined by measuring the amount of *p*-nitrophenol produced as described previously (*5*).

Microscopy Analyses. Samples from *S. cerevisiae* cells expressing the Pho84−GFP chimera in a Δ*gtr1* background grown in LP_i-defined medium were analyzed by fluorescence microscopy as described previously (*6*).

Determination of Protein Amounts. Protein was assayed by use of the commercially available Bio-Rad D_c protein assay kit (Bio-Rad), and bovine serum albumin was used as a standard.

RESULTS

Gtr1 and High-Affinity Phosphate Uptake. The Gtr1 is a soluble protein belonging to the Ras family of small G-binding proteins. Knowledge of its cellular role is emerging; Gtr1 appears to be a multifunctional protein that has been reported to be involved in nuclear trafficking (*26*), ribosome biogenesis (*16*), and high-affinity phosphate acquisition (*3*). In this study, we address the latter aspect. For this, a CEN.PK113-5D/Pho84^{WT}-MYC (*18*) strain devoid of the *GTR1* gene was constructed and compared with the *GTR1*$^+$ strain for high-affinity phosphate uptake capacity (Figure 1A) and extracellular acidic phosphatase activity (Figure 1B). Cells batch-cultivated in LP_i medium were collected at the indicated time points and analyzed for their ^{32}P uptake activity. A previous study has shown that the lack of the *GTR1* gene reduced the level of high-affinity phosphate uptake to ∼20% for yeast cells grown in phosphate-limited media (*3*). In that study, however, the phosphate uptake analysis was limited to cells grown to a specific optical density (A_{600} = 1.0). Under our experimental conditions, disruption of the *GTR1* gene influenced the growth rate of the strain to a minor extent with a moderate but significant

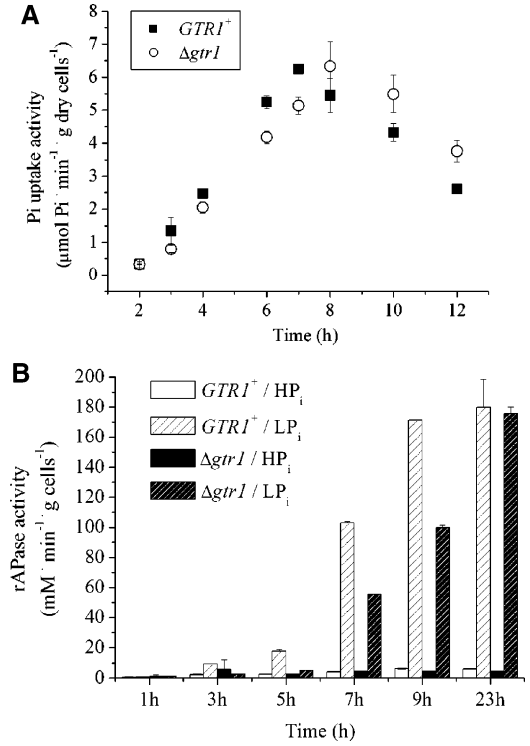

FIGURE 1: High-affinity phosphate uptake and phosphatase activity in Δ*gtr1* cells. The Pho84−MYC wild-type strain (*GTR1*$^+$) and the Δ*gtr1* mutant strain were grown aerobically under phosphate-limiting or phosphate-sufficient conditions. Cultures were sampled periodically for measurement of uptake of ^{32}P into *GTR1*$^+$ and Δ*gtr1* cells grown under phosphate-limiting conditions (A) and for measurements of the periplasmic acidic phosphatase (rAPase) activity of *GTR1*$^+$ and Δ*gtr1* cells grown under phosphate-limiting or phosphate-sufficient conditions (B) (see Experimental Procedures).

time-dependent delay in phosphate uptake response with maximal uptake activity of the *GTR1*$^+$ and the Δ*gtr1* cells seen at A_{600} values of 4.8 and 5.3, respectively (Figure 1A). However, both strains catalyze phosphate uptake to the same extent, with an activity in agreement with that previously reported for the Pho84 high-affinity transporter (*5*, *27*). Cells grown under phosphate-limiting conditions not only mobilize the derepressible Pho84 transporter to efficiently acquire phosphate from the environment but also enhance the expression and secretion of the Pho5 acidic phosphatase. This phosphatase activity allows for the scavenging of phosphate from phospho-moieties in the periplasmic compartment, which can then be translocated across the plasma membrane via the Pho84 transporter. Accordingly, *GTR1*$^+$ and Δ*gtr1* cells were cultivated in either HP_i or LP_i medium (Figure 1B). Both strains show a decreased phosphatase activity when grown in HP_i medium. However, the Pho5 activity is derepressed when the same cells are grown under phosphate-limiting conditions. Similar to what is seen for the high-affinity phosphate uptake response, a significant and even more pronounced time-dependent delay in upregulation of phosphatase activity was observed for Δ*gtr1* cells as compared to *GTR1*$^+$ cells grown under identical conditions. To further analyze the effects of the Gtr1 on the phosphate acquisition process, we investigated the *in vivo* consequences on Pho84 in a Δ*gtr1* background. For this, a functional Pho84−GFP chromosomal construct in the CEN.PK113-5D strain was created for the study of expression and *in vivo*

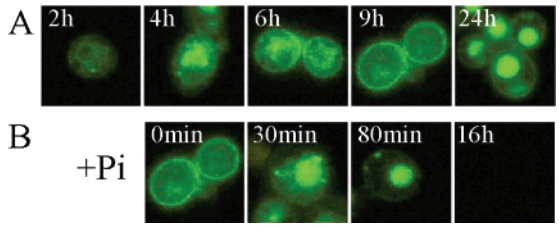

FIGURE 2: Cellular trafficking of the Pho84−GFP chimera in Δ*gtr1* cells. *In vivo* localization of the fluorescent Pho84−GFP chimera was analyzed in Δ*gtr1* cells collected during growth under phosphate-limiting conditions (A). Panel B shows the rapid internalization of the Pho84−GFP chimera in Δ*gtr1* cells to which phosphate at 10 mM, a repressible concentration, was added.

trafficking of the Pho84 protein under phosphate-limiting conditions (*6*, *18*) and under conditions of external phosphate supplementation. Analogous to wild-type cells expressing the Pho84−GFP chimera (*6*), Δ*gtr1* cells allow for a qualitatively comparable synthesis of the Pho84−GFP protein, where a maximum peripheral fluorescence is achieved after growth for 9 h in LP_i medium by transport-active cells (Figure 2). Upon exhaustion of available phosphate, the Pho84−GFP chimera expressed in wild-type *GTR1*$^+$ (*6*) and in Δ*gtr1* (Figure 2A) cells is endocytosed and transported to the vacuole for degradation. The analysis of Δ*gtr1* cells expressing the Pho84−GFP chimera reveals a wild-type-like response to exposure of repressible concentrations of phosphate, resulting in a fully depleted peripheral fluorescence within 30 min (Figure 2B).

Molecular Modeling of Gtr1. Gtr1 has been reported to be a member of a new, sixth subfamily of the Ras superfamily of small GTPases (*12*, *13*). Representative small G proteins from this superfamily were compared in a multiple-sequence alignment. The alignment shows the expected high level of conservation in the consensus motifs responsible for the specific interaction with guanine nucleotides, whereas the overall level of sequence identity of the G proteins is low (only ∼20−30%). On the basis of this analysis (kindly provided by K. Stengel and I. Sinning, data not shown), SRβ and Sar1 are identified as the closest relatives of Gtr1. Interestingly, Gtr1 seems to have a low GTPase activity as the purified protein is stable in the GTP-bound state (K. Stengel and I. Sinning, personal communication).

The cysteine mutations used in this study (EPR experiment; see below) were mapped onto a structural model of the Gtr1 G binding domain (Figure 3; the model was kindly provided by K. Stengel, I. Tews, and I. Sinning). The model shows that C62 is close to the G3 element, buried in the protein. C180 is located in the last helix of the G binding domain.

EPR Spectroscopy of Gtr1 Structure and Dynamics. The primary structure of Gtr1 contains the typical consensus motifs of G proteins (*12*, *13*). These conserved sequences are in the N-terminal part of Gtr1 (G domain, residues 1−185) (Figure 4A). To observe structure−function relationships in full-length and truncated Gtr1 mutants, a bacterial production system combined with a single purification step based on affinity chromatography was utilized. This yielded several milligrams of purified protein per liter culture with a protein purity of >90% (Figure 4B). Since nucleotide load analysis revealed a preference for GTP loading, GDP (200 μM) was included in the purification buffers, to increase the GDP−Gtr1 population for EPR analysis. We examined the EPR spectral changes upon addition of GTP to Gtr1 constructs spin labeled at one or more of the five native cysteines contained in the Gtr1 primary structure and also at two chosen locations (R37 and V67) that were mutated to cysteines in a cysteine-free Gtr1 background (Table 1 and Figure 4C−F). Sequence analysis of Gtr1 suggests two distinct domains, with the N-terminal half (residues 1−185) being homologous to the ras-like family of G proteins. We therefore examined the effects of GTP on spin-labels located in both halves of the protein (Figure 4C). The EPR spectra of spin-labels located in the Gtr1 N-terminal half (Figure 4C) report a conformational change in the presence of 1 mM nucleotide, whereas no change is observed from labels located in the C-terminal half (Figure 4C). This spectral change is specific for GTP, with ATP and also UTP and CTP producing spectra identical to that of Gtr1 alone. The line shape from each sample contains a mixture of weakly and strongly immobilized spin-labeled side chains (arrows, Figure 4), depending on the location of the label(s). In the presence of GTP, there is an increased side chain mobility seen in the N-terminal half, reflected by a sharper EPR line shape (Figure 4C). The spectral change suggests an increase in the population of weakly immobilized side chains when GTP is bound. Nearly all of this change is due to a mobilization at position C62, since spin-labeled single C180 does not report a significant change with GTP (Figure 4D).

As is evident in Figure 4D, the spectrum of residue C180 in the N-terminal portion of Gtr1 displays a broadening indicative of dipolar interaction between labels (*28*). The level of broadening indicates a self-association of the protein arranged such that the C180 sites are close to one another (within ∼15 Å). This association is consistent with the proposed oligomeric organization of Gtr1 (*13*).

To further probe the conformational dynamics associated with GTP binding, we selected two additional sites, R37 and V67, for nitroxide spin-label attachment. These sites were chosen because of their predicted proximity to the nucleotide-binding region within the N-terminal region. Thus, the single-Cys substitution R37C or V67C was introduced into the cysteine-free Gtr1 mutant, and the overexpressed proteins were spin-labeled and examined by EPR spectroscopy. As shown in Figure 4E, the nitroxide located at position 37 does not report a GTP-dependent change in conformational dynamics; however, position 67 reveals a significant broadening of the line shape when the protein is incubated with GTP in contrast to GDP. Thus, the side chain at position 67 becomes more restricted upon GTP binding.

Since changes in the side chain dynamics at C62 can report the binding of nucleotide, we used a spin-label at this position to explore the consequences of substituting residues within the conserved G4 motif (NKxD) (Figure 4A). In this motif, Gtr1 has a histidine in place of the conserved asparagine (H126, vs the consensus N126). Figure 5F shows the EPR signal given by the spin-label attached to C62 in the H126N (left panel) or H126K (right panel) mutant proteins. In the H126N mutant, GTP produces a similar but smaller line shape change, suggesting that H126 is not required for GTP binding. In contrast, the H126K substitution appears to have a significant effect on Gtr1 stability, as this mutation greatly increases the side chain motion of C62. Consistent with the

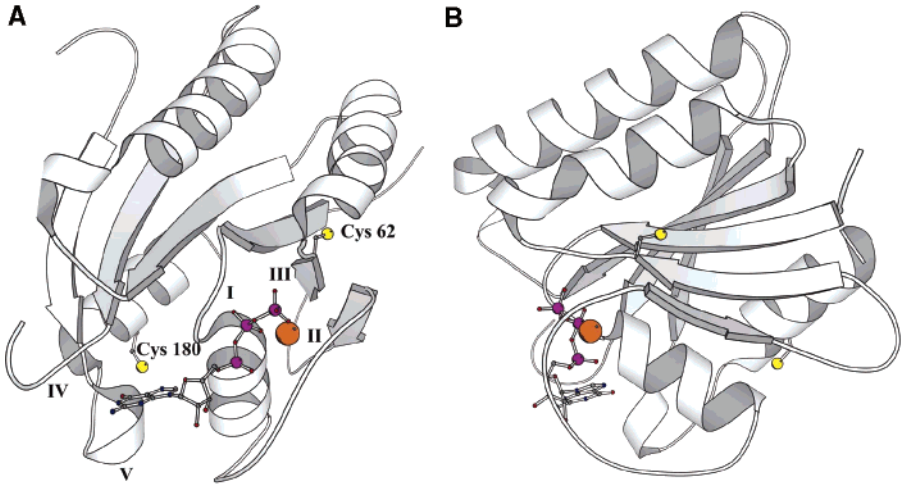

FIGURE 3: Structural modeling of the Gtr1. (A) A model of the G binding domain of Gtr1 is shown as a ribbon diagram (the model was kindly provided by K. Stengel, I. Tews, and I. Sinning). The consensus elements for nucleotide binding are marked with roman numerals (I−IV). The nucleotide (GTP) and the Mg^{2+} ion are shown in a ball-and-stick representation. Unstructured loop regions have been omitted. The two cysteine residues used in the EPR studies are shown with their side chains. The color code for the atoms is yellow for sulfur, blue for nitrogen, purple for phosphorus, and red for the Mg^{2+} ion. (B) Same as panel A but rotated by ~90°.

H126K mutation resulting in a structural alteration of this domain, the C62-labeled EPR spectrum of this mutant is unchanged when GTP is added in place of CTP.

DISCUSSION

The primary objectives of this work were to study the involvement of the soluble G protein, Gtr1, in high-affinity phosphate uptake in *S. cerevisiae* and to explore structural and functional aspects of this protein. The polytopic Pho84 protein is the major high-affinity phosphate transporter in *S. cerevisiae* and is responsible for a high-capacity uptake of inorganic phosphate in situations when the external phosphate supply is limited. In a previous study, the deletion of the *GTR1* gene was shown to severely impair the high-affinity phosphate uptake (*3*) with a resulting 80% activity reduction. That particular study was carried out on cells grown to an A_{600} of 1.0. In our comparative studies of *GTR1*$^+$ and Δ*gtr1* cells, with an intact and deleted *GTR1* gene, respectively, the phosphate uptake activity, localization of the Pho84 protein, and extracellular phosphatase activity were assayed at several time points during growth of cells in batch culture. Our qualitative analysis of localization and phosphate-mediated endocytosis of the Pho84−GFP chimera in a Δ*gtr1* background revealed no obvious changes as compared to *GTR1*$^+$ cells. Neither could the previously reported drastic impact of the absence of the *GTR1* on high-affinity phosphate uptake be seen, although a significant delay in the response was observed. This delay was also seen in the measurements of extracellular phosphatase activity levels. The reasons for the unexpected difference between the two independent studies are not fully understood, but differences such as yeast strain, growth medium, and growth conditions may contribute. The deletion of another *pho* gene, *PHO86*, with a phenotype similar to that of Δ*gtr1* (*29*), was shown to be important in the packaging of Pho84 molecules in COPII vesicles in the transport of the synthesized phosphate transporter from the ER to the Golgi (*30*). A similar function for Gtr1 cannot be excluded, although other modes of regulation are feasible as well. The apparent nonessential influence of Gtr1 in high-affinity phosphate uptake under the conditions that were studied implies that the absence of Gtr1 in Δ*gtr1* cells is counterbalanced by other factors such as proteins similar to Gtr1, by changes in transporter expression and/or turnover, or by an alternative regulatory pathway (see ref *31*).

The primary structure of the Gtr1 protein contains recognized guanine nucleotide binding motifs located in the N-terminal half of the protein (amino acids 1−185). Gtr1, together with its closest homologues, clusters apart from other known subclasses of the Ras superfamily of small G proteins, and is therefore considered to constitute a novel subclass. The obvious features of this subclass are an extended C-terminal domain and a histidine in the first position of the NKxD motif, which is associated with specificity for guanine nucleotides. Using EPR spectroscopy, we show that indeed the postulated G domain is sufficient for guanine nucleotide binding, implying that the C-terminal domain may have a regulatory function. The dipolar interaction observed with singly labeled C180 must arise from self-association of the protein. This interaction is seen also for the N-terminal domain only, thus showing that this part is sufficient for oligomerization of the Gtr1 molecule. Moreover, this observation is consistent with the structural model, which places the C180 side chain near the protein surface.

Of the native cysteines in both the C- and N-terminal domains, only C62 displays sensitivity to the nucleotide loading state. The spectral change is not seen with ATP and therefore appears to be specific for guanine nucleotides. C62 in Gtr1 is located within the G3 motif, and in our model, it is not facing toward the nucleotide-binding pocket. However, our data show that GTP-induced conformational changes can be monitored by EPR by introducing a spin-label at C62.

As mentioned above, Gtr1 is distinguished in part by its histidine residue at the first position of the NKxD guanine nucleotide-binding motif. The asparagine is highly conserved in other classes of the Ras G protein superfamily. Using the GTP binding sensitivity of the C62, we were able to conclude that the Gtr1 subgroup-specific histidine (H126) in the position of the asparagine in the G4 motif is not essential

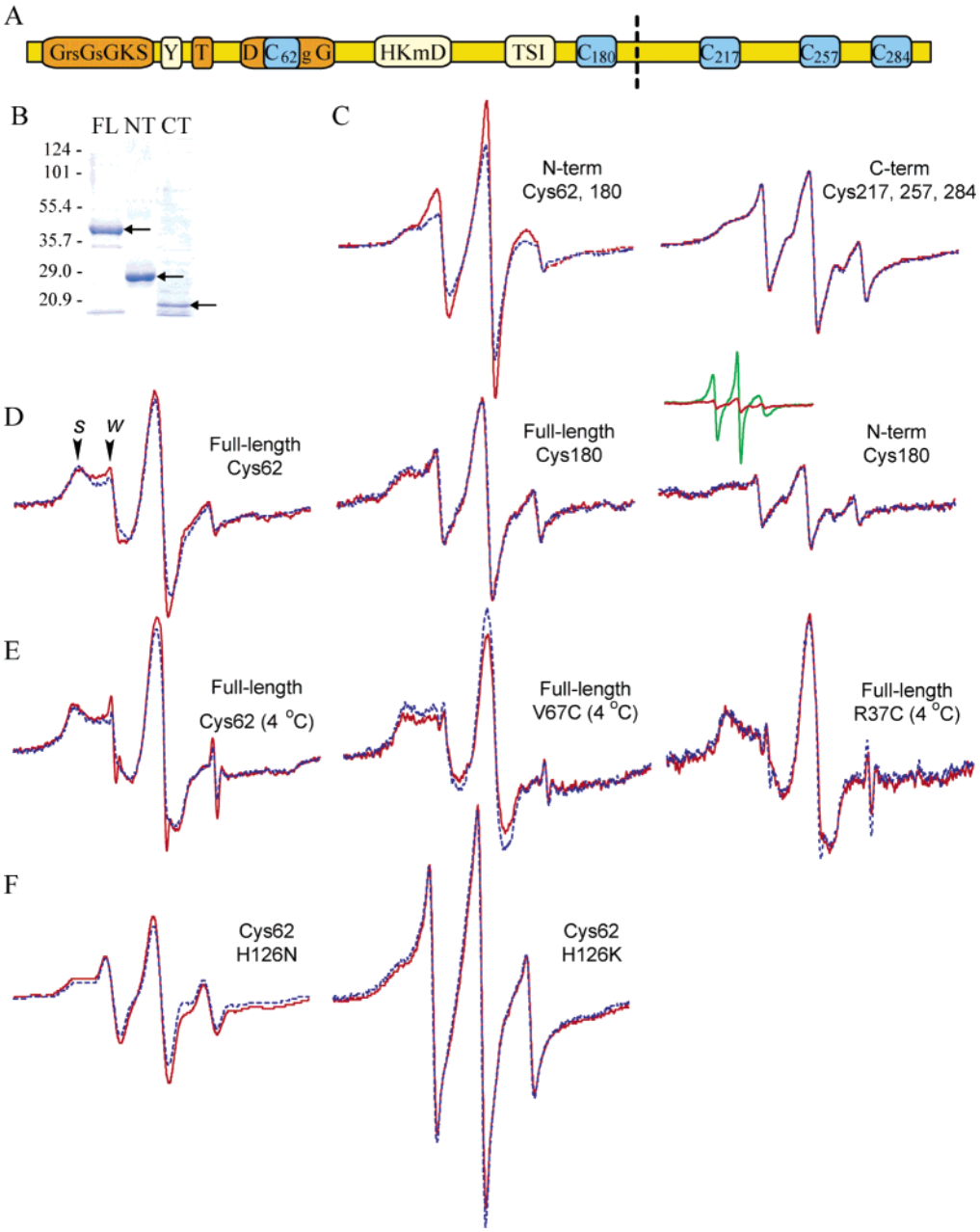

FIGURE 4: EPR spectroscopy of Gtr1 mutants. (A) Schematic presentation of the Gtr1 primary structure with phosphate/magnesium binding motifs (orange), guanine binding motifs (yellow), and native cysteines (blue). The dashed line in panel A indicates the site of separation between the N-terminal and C-terminal portions. The Coomassie Blue-stained SDS−polyacrylamide gel (B) shows the *E. coli*-produced and -purified full-length Gtr1 protein (FL, amino acids 1−310), the N-terminal portion of Gtr1 (NT, amino acids 1−185), and the C-terminal portion of Gtr1 (CT, amino acids 186−310). Site-directed mutants of the full-length and truncated forms of the Gtr1 protein were subjected to nitroxide spin labeling of cysteine residues and analyzed by EPR spectroscopy in the absence (dashed blue line) or presence (red line) of 1 mM GTP (C−F). The low-field line resolves two distinct populations in each sample, a broad line indicating strongly immobilized side chains (*s* in panel D) and a weakly immobilized population with greater motional freedom (*w* in panel D). GTP increases the motion of nitroxides attached to C62. In panel C, the spectra from spin-labels attached to the native cysteines in the N-terminal (C62 and C180, left) and C-terminal (C217, C257, and C284, right) halves of Gtr1. The individual cysteines C62 (full-length, left panel) and C180 (full-length form in the middle panel and N-terminal portion in the right panel) are analyzed in panel D. In panel E, the labels at C62 (left panel) and also at R67C (middle panel) and V37C (right panel) are analyzed at a low temperature (4 °C). The role of the histidine in the HKmD motif was analyzed in panel F, in a C62-labeled protein. The left panel shows the spectra of the H126N mutant, and the right panel shows the corresponding spectra for the H126K mutant. For all pairs, the CTP and GTP spectra were acquired on identical sample amounts and instrument settings. The protein concentrations were 16 μM (i.e., 62-fold excess of nucleotides) for all full-length Gtr1 mutants and 26 μM (i.e., 39-fold excess of nucleotides) and 35 μM (i.e., 28-fold excess of nucleotides) for the N- and C-terminal portions, respectively. Spectra are normalized to the amplitude of the unfolded protein (1% SDS; see the green line in panel D).

for GTP binding. This was seen with an amino acid exchange for asparagine. A lysine at the same position results in a significant increase in the population of C62 side chains with high mobility, suggesting the H126K mutation has a destabilizing effect on the Gtr1 structure.

To date, no GTPase activity has been demonstrated for Gtr1 (see, for example, ref *13*). However, the possibility of enhanced GTP hydrolysis in the yeast cells activated by different factors, for example, GTPase-activating proteins, cannot be excluded.

ACKNOWLEDGMENT

Brian Soldavini (University of California, Davis, CA) is greatly acknowledged for excellent technical assistance. Katharina Stengel, Ivo Tews, and Irmi Sinning (Biochemie-Zentrum, Heidelberg, Germany) are gratefully acknowledged for providing a structural model of the Gtr1 G binding domain and for nucleotide load analysis. We thank Irmi Sinning (Biochemie-Zentrum) for valuable suggestions and critical comments about the manuscript.

REFERENCES

1. Persson, B. L., Lagerstedt, J. O., Pratt, J. R., Pattison-Granberg, J., Lundh, K., Shokrollahzadeh, S., and Lundh, F. (2003) Regulation of phosphate acquisition in *Saccharomyces cerevisiae*, *Curr. Genet. 43*, 225−244.
2. Bun-ya, M., Nishimura, M., Harashima, S., and Oshima, Y. (1991) The PHO84 gene of *Saccharomyces cerevisiae* encodes an inorganic phosphate transporter, *Mol. Cell. Biol. 11*, 3229−3238.
3. Bun-ya, M., Harashima, S., and Oshima, Y. (1992) Putative GTP-binding protein, Gtr1, associated with the function of the Pho84 inorganic phosphate transporter in *Saccharomyces cerevisiae*, *Mol. Cell. Biol. 12*, 2958−2966.
4. Pao, S. S., Paulsen, I. T., and Saier, M. H., Jr. (1998) Major facilitator superfamily, *Microbiol. Mol. Biol. Rev. 62*, 1−34.
5. Martinez, P., Zvyagilskaya, R., Allard, P., and Persson, B. L. (1998) Physiological regulation of the derepressible phosphate transporter in *Saccharomyces cerevisiae*, *J. Bacteriol. 180*, 2253−2256.
6. Petersson, J., Pattison, J., Kruckeberg, A. L., Berden, J. A., and Persson, B. L. (1999) Intracellular localization of an active green fluorescent protein-tagged Pho84 phosphate permease in *Saccharomyces cerevisiae*, *FEBS Lett. 462*, 37−42.
7. Berhe, A., Fristedt, U., and Persson, B. L. (1995) Expression and purification of the high-affinity phosphate transporter of *Saccharomyces cerevisiae*, *Eur. J. Biochem. 227*, 566−572.
8. Fristedt, U., Weinander, R., Martinsson, H. S., and Persson, B. L. (1999) Characterization of purified and unidirectionally reconstituted Pho84 phosphate permease of *Saccharomyces cerevisiae*, *FEBS Lett. 458*, 1−5.
9. Fristedt, U., van der Rest, M., Poolman, B., Konings, W. N., and Persson, B. L. (1999) Studies of cytochrome *c* oxidase-driven H^+-coupled phosphate transport catalyzed by the *Saccharomyces cerevisiae* Pho84 permease in coreconstituted vesicles, *Biochemistry 38*, 16010−16015.
10. Sprang, S. R. (1997) G protein mechanisms: Insights from structural analysis, *Annu. Rev. Biochem. 66*, 639−678.
11. Kjeldgaard, M., Nyborg, J., and Clark, B. F. C. (1996) The GTP binding motif: Variations on a theme, *FASEB J. 10*, 1347−1368.
12. Schürmann, A., Brauers, A., Massmann, S., Becker, W., and Joost, H.-G. (1995) Cloning of a novel family of mammalian GTP-binding proteins (RagA, RagBs, RagB1) with remote similarity to the Ras-related GTPases, *J. Biol. Chem. 270*, 28982−28988.
13. Nakashima, N., Noguchi, E., and Nishimoto, T. (1999) *Saccharomyces cerevisiae* putative G protein, Gtr1p, which forms complexes with itself and a novel protein designated as Gtr2p, negatively regulates the Ran/Gsp1p G protein cycle through Gtr2p, *Genetics 152*, 853−867.
14. Hirose, E., Nakashima, N., Sekiguchi, T., and Nishimoto, T. (1998) RagA is a functional homologue of *S. cerevisiae* Gtr1p involved in the Ran/Gsp1-GTPase pathway, *J. Cell Sci. 111*, 11−21.
15. Nakashima, N., Hayashi, N., Noguchi, E., and Nishimoto, T. (1996) Putative GTPase Gtr1p genetically interacts with the RanGTPase cycle in *Saccharomyces cerevisiae*, *J. Cell Sci. 109*, 2311−2318.
16. Sekiguchi, T., Todaka, Y., Wang, Y., Hirose, E., Nakashima, N., and Nishimoto, T. (2004) A novel human nucleolar protein, Nop132, binds to the G proteins, RRAG A/C/D, *J. Biol. Chem. 279*, 8343−8350.
17. Zanchin, N. I., and Goldfarb, D. S. (1999) Nip7p interacts with Nop8p, an essential nucleolar protein required for 60S ribosome biogenesis, and the exosome subunit Rrp43p, *Mol. Cell. Biol. 19*, 1518−1525.
18. Lagerstedt, J. O., Zvyagilskaya, R., Pratt, J. R., Pattison-Granberg, J., Kruckeberg, A. L., Berden, J. A., and Persson, B. L. (2002) Mutagenic and functional analysis of the C-terminus of *Saccharomyces cerevisiae* Pho84 phosphate transporter, *FEBS Lett. 526*, 31−37.
19. De Antoni, A., and Gallwitz, D. (2000) A novel multi-purpose cassette for repeated integrative epitope tagging of genes in *Saccharomyces cerevisiae*, *Gene 246*, 179−185.
20. Gietz, R. D., and Woods, R. A. (2002) Transformation of yeast by lithium acetate/single-stranded carrier DNA/polyethylene glycol method, *Methods Enzymol. 350*, 87−96.
21. Kaneko, Y., Toh-e, A., and Oshima, Y. (1982) Identification of the genetic locus for the structural gene and a new regulatory gene for the synthesis of repressible alkaline phosphatase in *Saccharomyces cerevisiae*, *Mol. Cell. Biol. 2*, 127−137.
22. Froncisz, W., and Hyde, J. S. (1982) The loop-gap resonator: A new microwave lumped circuit ESR sample structure, *J. Magn. Reson. 47*, 515−521.
23. Hubbell, W. L., Froncisz, W., and Hyde, J. S. (1987) Continuous and stopped flow electron-paramagnetic-res spectrometer based on a loop gap resonator, *Rev. Sci. Instrum. 58*, 1879−1886.
24. Laemmli, U. K., Beguin, F., and Gujer-Kellenberger, G. (1970) A factor preventing the major head protein of bacteriophage T4 from random aggregation, *J. Mol. Biol. 47*, 69−85.
25. Nyrén, P., Nore, B. F., and Baltscheffsky, M. (1986) Studies of photosynthetic inorganic pyrophosphate formation in *Rhodospirillum rubrum* chromatofores, *Biochim. Biophys. Acta 851*, 276−282.
26. Sekiguchi, T., Hirose, E., Nakashima, N., Ii, M., and Nishimoto, T. (2001) Novel G proteins, Rag C and Rag D, interact with GTP-binding proteins, Rag A and Rag B, *J. Biol. Chem. 276*, 7246−7257.
27. Pattison-Granberg, J., and Persson, B. L. (2000) Regulation of cation-coupled high-affinity phosphate uptake in the yeast *Saccharomyces cerevisiae*, *J. Bacteriol. 182*, 5017−5019.
28. Altenbach, C., Oh, K. J., Trabanino, R. J., Hideg, K., and Hubbell, W. L. (2001) Estimation of inter-residue distances in spin labeled proteins at physiological temperatures: Experimental strategies and practical limitations, *Biochemistry 40*, 15471−15482.
29. Yompakdee, C., Bun-ya, M., Shikata, K., Ogawa, N., Harashima, S., and Oshima, Y. (1996) A putative new membrane protein, Pho86p, in the inorganic phosphate uptake system of *Saccharomyces cerevisiae*, *Gene 171*, 41−47.
30. Lau, W. T., Howson, R. W., Malkus, P., Schekman, R., and O'Shea, E. K. (2000) Pho86p, an endoplasmic reticulum (ER) resident protein in *Saccharomyces cerevisiae*, is required for ER exit of the high-affinity phosphate transporter Pho84p, *Proc. Natl. Acad. Sci. U.S.A. 97*, 1107−1112.
31. Raamsdonk, L. M., Teusink, B., Broadhurst, D., Zhang, N., Hayes, A., Walsh, M. C., Berden, J. A., Brindle, K. M., Kell, D. B., Rowland, J. J., Westerhoff, H. V., van Dam, K., and Oliver, S. G. (2001) A functional genomics strategy that uses metabolome data to reveal the phenotype of silent mutations, *Nat. Biotechnol. 19*, 45−50.

BI048659V